Korean J Physiol Pharmacol
Vol 13: 61−70, February, 2009

Multiple Residues in the P-Region and M2 of Murine Kir 2.1 Regulate Blockage by External Ba^{2+}

Young Mee Lee[1,†], Gareth A. Thompson[3,†], Ian Ashmole[2], Mark Leyland[4], Insuk So[1,*], and Peter R. Stanfield[2]

[1]Department of Physiology and Biophysics, Seoul National University, College of Medicine, Seoul 110-799, Korea, [2]Department of Biological Sciences, University of Warwick, Coventry CV4 7AL; Ion Channel Group, [3]Department of Cell Physiology & Pharmacology, University of Leicester, PO Box 138, Leicester, LE1 9HN, UK, [4]Department of Biochemistry, University of L:eicester, LE1 7RH, UK

We have examined the effects of certain mutations of the selectivity filter and of the membrane helix M2 on Ba^{2+} blockage of the inward rectifier potassium channel, Kir 2.1. We expressed mutant and wild type murine Kir 2.1 in Chinese hamster ovary (CHO) cells and used the whole cell patch-clamp technique to record K^+ currents in the absence and presence of externally applied Ba^{2+}. Wild type Kir2.1 was blocked by externally applied Ba^{2+} in a voltage and concentration dependent manner. Mutants of Y145 in the selectivity filter showed little change in the kinetics of Ba^{2+} blockage. The estimated $K_d(0)$ was 108 μM for Kir2.1 wild type, 124 μM for a concatameric WT-Y145V dimer, 109 μM for a WT-Y145L dimer, and 267 μM for Y145F. Mutant channels T141A and S165L exhibit a reduced affinity together with a large reduction in the rate of blockage. In S165L, blockage proceeds with a double exponential time course, suggestive of more than one blocking site. The double mutation T141A/S165L dramatically reduced affinity for Ba^{2+}, also showing two components with very different time courses. Mutants D172K and D172R (lining the central, aqueous cavity of the channel) showed both a decreased affinity to Ba^{2+} and a decrease in the *on* transition rate constant (k_{on}). These results imply that residues stabilising the cytoplasmic end of the selectivity filter (T141, S165) and in the central cavity (D172) are major determinants of high affinity Ba^{2+} blockage in Kir 2.1.

Key Words: Potassium channel, Inward rectifier, Ionic selectivity, Barium blockage

INTRODUCTION

Kir channels are expressed by a host of mammalian cell types. Their best known functions include the setting of resting membrane potentials and control of cellular excitability (for review, see Stanfield et al., 2002). Kir channels perform these roles by allowing K^+ ions to flow at membrane potentials close to the equilibrium potential for K^+ (E_K). However, channels are gated by intracellular Mg^{2+} (Matsuda et al., 1987) and polyamines (Ficker et al., 1994; Fakler et al., 1994, 1995; Lopatin et al., 1994, 1995) and close under sufficient depolarization. Gating by Mg^{2+} and polyamines also results in channels being opened by an increase in extracellular [K^+] (Hagiwara and Yoshii, 1979; Leech and Stanfield, 1981; Lopatin and Nichols, 1996). Functional Kir channels form as homo- or heterotetramers (Yang et al., 1995), each channel subunit possessing two membrane-spanning regions (M1 and M2) with a pore-forming loop between them (the P or H5 region; e.g. Kubo et al., 1993; see Stanfield et al., 2002; Kuo et al., 2003; Nishida et al., 2007; for review).

The ability of Ba^{2+} to block native inward rectifier K^+ channels has been known for some time (Hagiwara et al., 1978; Standen and Stanfield, 1978). This characteristic has resulted in Ba^{2+} being used extensively in the separation of Kir currents in native membranes (see Stanfield et al., 2002). Inevitably, more detailed investigations of how Ba^{2+} blocks cloned Kir channels, including the rat epithelial channel Kir 1.1 (ROMK2, Zhou et al., 1996) and mouse macrophage channel Kir 2.1 (IRK1, Shieh et al., 1998), have followed.

Residues lining the pore of Kir channels contribute to blockage by Ba^{2+}; these residues include those at the outer mouth of the pore and those forming the selectivity filter. Previous work has shown that a highly conserved arginine residue, located in the outer vestibule at position 148 in Kir2.1, forms a barrier for external cations (Sabirov et al., 1997). Kir 7.1 lacks this Arg residue, and its replacement by Met accounts for a very low affinity for Ba^{2+} (Doring et al., 1998; Krapivinsky et et al., 1998). The presence of a glutamate at position 125 (also part of the outer vestibule) in Kir2.1 was shown to affect both Ba^{2+} sensitivity and single- channel conductance (Navaratnam et al., 1995; Topert et al., 1998).

*Corresponding to: Insuk So, Department of Physiology and Biophysics, Seoul National University, College of Medicine, 28 Yonggon-dong, Chongno-gu, Seoul 110-799, Korea. (Tel) 82-2-740-8228, (Fax) 82-2-763-9667, (E-mail) p.r.stanfield@warwick.ac.uk or insuk@plaza.snu.ac.kr

†YM Lee and GA Thompson contributed equally to this work and should be considered as joint first author.

ABBREVIATIONS: CHO, Chinese hamster ovary; WT, wild type; Kir channel, inward rectifier K channel.

Involvement of the filter itself was shown in Kir2.1 by mutations replacing certain peptide bonds by ester bonds, removing backbone amide groups from parts of the selectivity filter. Such mutation of the inner glycine in the signature motif GYG decreased binding affinity for Ba^{2+} 6500-fold (Lu et al., 2001). Secondly, Zhou et al. (1996) demonstrated that differences in the characteristics of Ba^{2+} blockage of Kir 1.1 and 2.1 could be attributed in part to the presence of a valine residue (Val121) in the P-region of Kir 1.1; this residue aligns with a threonine (Thr141) in Kir 2.1. The mutant channel Kir 1.1 (V121T) exhibited a ten-fold increase in Ba^{2+} affinity. In Kir2.1, Alagem et al. (2001) implicated Thr141 as a determinant of Ba^{2+} blockage. Involvement of the pore helix was demonstrated in Kir3.0 by Lancaster et al. (2000), who showed that mutation of residues of Kir3.1/3.4 heteromers (F137S and E139Q in Kir3.1 and E145Q in Kir3.4) produced substantial decreases in Ba^{2+} sensitivity. Thus residues lining the selectivity filter, or stabilising the structure of the filter, appear to affect Ba^{2+} blockage.

In the bacterial channel KcsA, crystallography suggests that the Ba^{2+} blocking site is indeed in the filter, in the innermost K^+ coordination site (S4), the site immediately adjacent to the central cavity (Jiang and MacKinnon, 2000). Such a blocking site will mean that Ba^{2+} must pass through most of the selectivity filter (K^+ coordination sites S1 to S3) to block the channel. As Jiang and MacKinnon (2000) suggest, K^+ ions occupying these sites will affect blockage, essentially trapping Ba^{2+} in its blocking site (S4; see also Neyton and Miller, 1988a, b). K^+ ions occupying the central cavity − beyond the selectivity filter − may also affect blockage forming an 'internal lock-in site' (Jiang and MacKinnon, 2000).

The central cavity is lined by M2 (Minor et al., 1999; see also Stanfield et al., 2002; Nishida et al., 2007). A crucial residue in this part of the structure is Asp172 (Stanfield et al., 1994; So et al., 2003a, b), which is closely involved in gating of channels by Mg^{2+} and polyamines (for review, see Stanfield et al., 2002) and important in coordinating K^+ in this central cavity. The residue has also been shown to form part of an internal selectivity filter (Abrams et al., 1996; Reuveny et al., 1996). In Kir 3.1/3.4 heteromers, the Kir3.4 mutant N179D−N179 is in the position equivalent to D172 in Kir2.1 - increased sensitivity to Ba^{2+} (Lancaster et al., 2000).

We have previously identified certain residues in the pore (P-)region (Thr141) and M2 (Ser165) of Kir2.1 which influence the ability of Cs^+ and Rb^+ to block or permeate the channel (Thompson et al., 2000a). We ask whether these results are emulated by Ba^{2+} blockage. Since we have also shown that Y145 mutants express well in monomeric form (Y145F) or in a concatameric dimer (WT-Y145 mutant), where only two of the four Tyr residues in the (tetrameric) channel are replaced (So et al., 2001), we investigate effects of these mutants on Ba^{2+} blockage. We also ask whether Asp172 contributes significantly to Ba^{2+} blockage.

Some of this work has been published in abstract form (Thompson et al., 1998; Thompson et al., 2000b; Lee et al., 2001).

METHODS

Chinese hamster ovary (CHO) cells were cultured in minimum essential medium alpha (Gibco) supplemented with 10% (w/v) fetal calf serum. Site-directed mutagenesis of murine Kir 2.1 was using the method of Kunkel (1985). Mutations were verified by sequencing the entire Kir2.1 coding sequence. Use of a concatameric dimer, permitting mutation of residues in only one of the two conjoined subunits, has been described before (Dart et al., 1998). Wild type or mutant Kir 2.1 cDNA was subcloned into the vector pCDNA3 and co-transfected with a plasmid containing the cDNA for Enhanced Green Fluorescent Protein (EGFP) as a transfection marker, using FuGENE^{TM} 6 transfection reagent (Roche). Successfully transfected cells were identified 24-48 hours later under fluorescence microscopy.

Whole-cell currents were recorded using an Axopatch 200A amplifier (Axon Instruments). Currents were filtered at 5 kHz (-3dB, 4-pole Bessel), digitized using frequencies ranging from 0.1～10 kHz using a Digidata 1,200 interface (Axon Instruments), and analysed on a Pentium PC using software written by Dr NW Davies (Cell Physiology and Pharmacology, University of Leicester). The pipette (intracellular) solution contained (mM): HEPES, 10; EDTA, 10; K^+ (as KCl & KOH), 140; pH adjusted to 7.2 with KOH. External solutions contained (mM): HEPES, 10; KCl, 70; N-methyl-D-glucamine (NMDG), 70; $CaCl_2$, 2; $MgCl_2$, 2; pH adjusted to 7.2 with HCl. Where Ba^{2+} concentrations greater than 300 μM were required, NMDG chloride was replaced with $BaCl_2$ to maintain osmolarity. The calculated junction potential between the pipette (140 mM K^+) and bath (70 mM K^+) solutions used with all cells during sealing was 4.1 mV (pipette negative; using the program JPCalc, PH Barry, University of New South Wales). No correction was applied for this junction potential.

Experiments were carried out at room temperature (18～22°C). A multi-line gravity driven perfusion system was used to apply different solutions to individual cells under whole cell clamp. Results are given as means±s.e.m. Where appropriate, results were compared using Student's t test.

RESULTS

The blockage of Kir2.1 by extracellular Ba^{2+}

Ba^{2+} blocks wild type Kir2.1 channels in a voltage-, concentration-, and time-dependent manner. Fig. 1 shows current traces recorded from a CHO cell expressing the gene for Kir2.1 in the absence and in the presence of Ba^{2+} at the concentrations indicated. The extent of blockage by Ba^{2+} increased at more negative membrane potential and with increasing $[Ba^{2+}]_o$. Fig. 2A shows, from left to right, the dose-response curves for the blockage of the steady-state Kir currents by extracellular Ba^{2+} at −127, −117, −97, −77, and −57 mV. The dose-response curves illustrate the voltage-dependent inhibition of Kir currents by extracellular Ba^{2+}. The dose-response curves at each potential were described by the equation (Eqn 1):

$$I_{frac} = \left\{1 + \left(\frac{[Ba^{2+}]}{K_d(V)}\right)^n\right\}^{-1} \quad (1)$$

where I_{frac} is the current remaining at steady-state, in the presence of $[Ba^{2+}]_o$, K_d(V) is the dissociation constant, which depends on voltage (see below), and n is the Hill coefficient (assumed to be 1).

With the addition of Ba^{2+} at micromolar concentrations, K^+ currents decay with a single order exponential time

course (time constant τ ms) to a steady state level (Fig. 1). The simplest scheme explaining such kinetics is given below:

$$R + Ba^{2+} \underset{k_{off}}{\overset{k_{on}}{\rightleftharpoons}} R.Ba^{2+} \quad (2)$$

where R is the ion channel, $R.Ba^{2+}$ is the blocked channel, complexed with Ba^{2+}, and k_{on} and k_{off} are transition rate constants. The validity of this scheme was tested by fitting the blocking rate ($1/\tau$) for each voltage against [Ba^{2+}] (Fig. 2B). The rate increased (τ decreased) with increasing [Ba^{2+}] at a given membrane potential and with membrane hyperpolarization. With 30 μM Ba^{2+}, the mean time constants (τ) were 30.5 ± 6.7 ms at −127 mV, 42.5 ± 9.7 ms at −117 mV, 81.8 ± 19.9 ms at −97 mV, 144.4 ± 44.0 ms at −77 mV, and 221.8 ± 54.7 ms at −57 mV (n=5, mean ± s.e.m.). The time constant is related to the transition rate constants k_{on} and k_{off} and to the Ba^{2+} concentration by the relationship:

$$\frac{1}{\tau} = k_{on} \cdot [Ba^{2+}]_o + k_{off} \quad (3)$$

Good linear fits (providing a slope equal to k_{on} and an intercept on the $1/\tau$ axis of k_{off}) were obtained for wild type Kir2.1, indicating that the kinetics for the blockage of the wild type channel is indeed first order (Eqn 2; Fig. 2B). k_{on} values were obtained from the value of τ by fitting regression lines to Eqn (3), whereas k_{off} values were obtained using K_d and k_{on} ($K_d = k_{off}/k_{on}$). k_{on}, increased with hyperpolarization (Fig. 3A), while k_{off} changed little between −127 and −57 mV (Fig. 3B). The interaction of Ba^{2+} with its binding site in the Kir2.1 channels (Fig. 3C) acquires its voltage dependence principally from the voltage dependence of k_{on}.

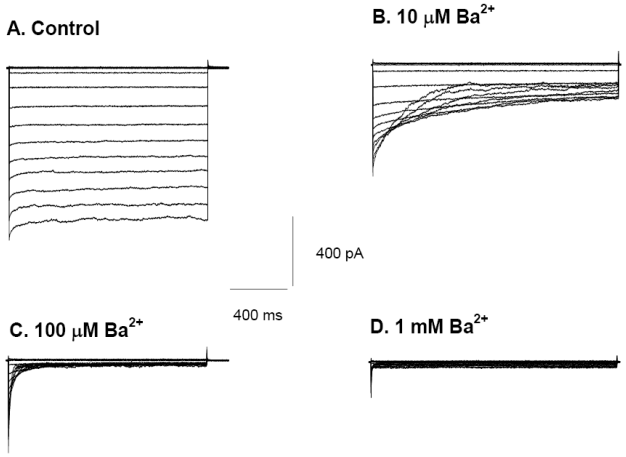

Fig. 1. Ba^{2+} blockage of wild type Kir2.1 channels. (A) Membrane currents recorded from a single CHO cell expressing the gene for Kir2.1 in response to voltage steps from a holding potential of −17 mV to test potentials ranging from +63 mV to −117 mV, using 10 mV increments. Extracellular [K^+] was 70 mM, and intracellular [K^+] was 140 mM. (B∼D) K^+ currents activated by voltage steps from −17 mV to a range of potentials between +63 and −127 mV, in the presence of 10 μM (B), 100 μM (C), 1 mM (D) $[Ba^{2+}]_o$. The current was reduced to 3.8±0.6% of control levels after 1,500 ms at −117 mV in the presence of 100 μM Ba^{2+} (n=7).

Ba^{2+} blockage of Y145 mutants

Kv and Kir channels have a highly homologous sequence T(S)xxTxGY(F)G within the pore region. This K^+ channel signature sequence acts as a common catalytic domain that determines the ion selectivity and permeation characteristics of K^+ channels (Heginbotham et al., 1994; Doyle et al., 1997; Nishida et al., 2007) and we investigated alterations of its structure on Ba^{2+} blockage. We replaced the tyrosine residue in GYG in two of the four channel subunits forming each channel molecule by valine (WT-Y145V) or by Leu (WT-Y145L), as in certain forms of K_{2P} (*e.g.* TWIK-1; Lesage et al., 1996). We also tested the effects of replacing Tyr by Phe, (giving GFG as *e.g.* in P1 of the K_{2P} channel TASK-1; Duprat et al., 1997). These changes however do not affect ionic selectivity or unitary conductance in Kir2.1 (So et al., 2001).

In Fig. 3A the values for the transition rate constant k_{on} are plotted as functions of the membrane potential. Values of k_{on} showed little change from those seen in wild type

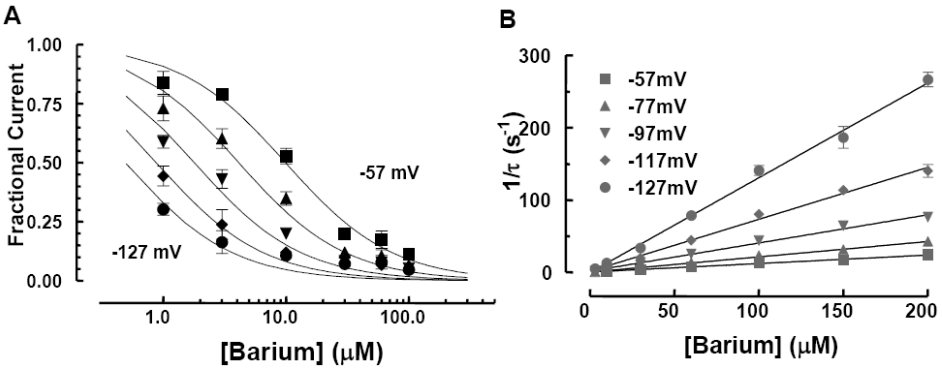

Fig. 2. Voltage and concentration dependence of blockage by $[Ba^{2+}]_o$ of Kir2.1. (A) Dose-response curves for extracellular Ba^{2+} blockage of steady-state I_K at −57 mV (squares), −77 mV (triangles), −97 mV (inverted triangles), −117 mV (diamonds), −127 mV (circles). Lines are the best fits to the averaged data (n=7 for each point) using the Hill equation (Eqn. 1 of text). (B) The reciprocal of the time constant (τ) of exponential curves fitted to development of Ba^{2+} blockage plotted against Ba^{2+} concentration (n=5). Solid lines are linear fits to data using Eqn (3) of the text. Slopes (bottom to top) at −57 mV (squares), −77 mV (triangles), −97 mV (inverted triangles), −117 mV (diamonds), −127 mV (circles) were: 1.1×10^5 $M^{-1}s^{-1}$, 1.9×10^5 $M^{-1}s^{-1}$, 3.9×10^5 $M^{-1}s^{-1}$, 6.4×10^5 $M^{-1}s^{-1}$ and 9.1×10^5 $M^{-1}s^{-1}$, respectively.

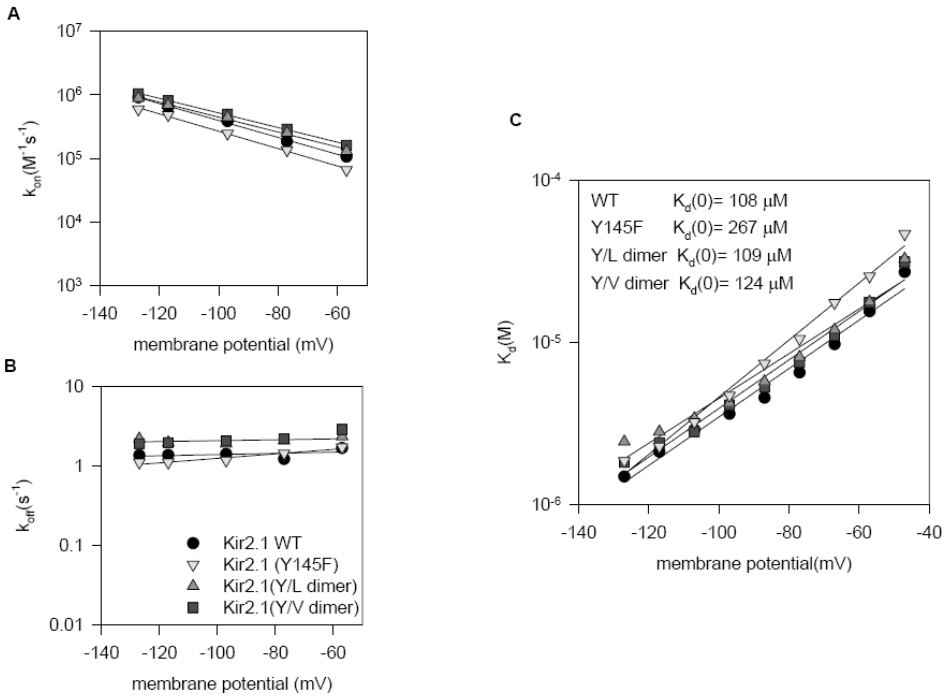

Fig. 3. Blockage by Ba^{2+} is similar in Kir2.1 wild type, Y145F, WT-Y145L dimer and WT-Y145V dimer. (A) Plot of k_{on} against membrane potential for wild type and Y145 mutants. k_{on} values were obtained from the value of τ by fitting regression lines to Eqn (3). (B) Plot of k_{off} against membrane potential for wild type and for Y145 mutants. k_{off} values were obtained using K_d and k_{on}. (C) K_d values obtained from the concentration-dependent inhibition of the steady-state currents were plotted against membrane potential. The solid line is the best fit of the data obtained at membrane potential (V) ranging from −127 mV to −47 mV, using the Woodhull equation (Eqn 4 of text).

Table 1. Ba^{2+} blockage in wild type and in mutant channels

Channel mutant	$K_d(0)$ (μM)	δ	k_{on} (−127 mV) ($M^{-1}s^{-1}$)	k_{off} (−127 mV) (s^{-1})
Kir2.1-WT	108	0.43	9.1×10^5	1.35
WT-Y145V dimer	124	0.43	1.0×10^6	1.89
WT-Y145L dimer	109	0.40	8.9×10^5	2.85
Y145F	267	0.51	5.9×10^5	1.10
T141A	858	0.57	9.5×10^4	
S165L	1,040	0.69	1.6×10^4	
T141A/S165L	473,000	1.08		
D172K	2,500	0.42	1.3×10^4	0.54
D172R	1,800	0.49	6.4×10^4	0.91

$K_d(0)$ is the dissociation constant at 0 mV and δ is the electrical distance between the outside of the membrane and the blocking site, both obtained using Eqn (4) of the text. The values for the transition rate constants k_{on} and k_{off} are derived using Eqn (3) of the text and are given here for a membrane potential of −127 mV.

(Table 1). To assay the voltage dependence of inhibition of Kir currents by $[Ba^{2+}]_o$, the K_d values obtained from the blockage of Kir currents were plotted against the membrane potential (Fig. 3C). The solid line is the fit to the data points from −47 to −127 mV, using the model of Woodhull (1973):

$$K_d(V) = K_d(0).\exp\left\{\frac{z\delta VF}{RT}\right\} \quad (4)$$

where $K_d(0)$ is the dissociation constant at 0 mV, z is the valence of the blocking ion, δ is the electrical distance from outside to the blocking site, and *V, F, R,* and *T* have their usual meanings. The estimated $K_d(0)$ was 108 μM for Kir2.1 wild type, 124 μM for the WT-Y145V dimer, 109 μM for the WT-Y145L dimer, and 267 μM for Y145F. The electrical distances, δ, that were obtained from the fit were also similar to wild type (Table 1).

Mutation T141A alters blockage by Ba^{2+}

When the threonine residue at position 141 was replaced by alanine (T141A), the characteristics of block by Ba^{2+} were altered significantly (Fig. 4). The rate of block was slowed dramatically, while the $K_d(0)$ was increased to 858 ± 62 μM and δ was 0.57. Examination of the apparent k_{on} and k_{off} in T141A showed the change in affinity to be predominantly the result of a 10-fold decrease in k_{on} at all voltages examined accompanied by a smaller reduction in k_{off}. Such effects are consistent with the work of Zhou et al. (1994) in Kir1.1.

Mutant S165L shows two components of block

We next considered the effect of S165L on blockage by Ba^{2+}. In the mutant channel, $K_d(0)$ was increased to 1.04 mM and δ was 0.69 (Table 1). Scrutiny of the time-course of blockage at Ba^{2+} concentrations (>100 μM) showed it to occur with two components; these 'fast' and 'slow' components of blockage were each an exponential function of time (Fig. 5). By plotting $1/\tau$ against a range of external Ba^{2+} concentrations it is possible to identify that the single component seen at low Ba^{2+} concentrations (<100 μM) is equivalent to the slow component observed with higher concentrations. Further analysis of Ba^{2+} blockage in this mutant channel was made difficult because the two components of blockage could be dissected over only a narrow concentration range, a difficulty compounded by the relatively high affinity of the channel for Ba^{2+}.

In a previous study of Cs^+ and Rb^+ blockage (Thompson

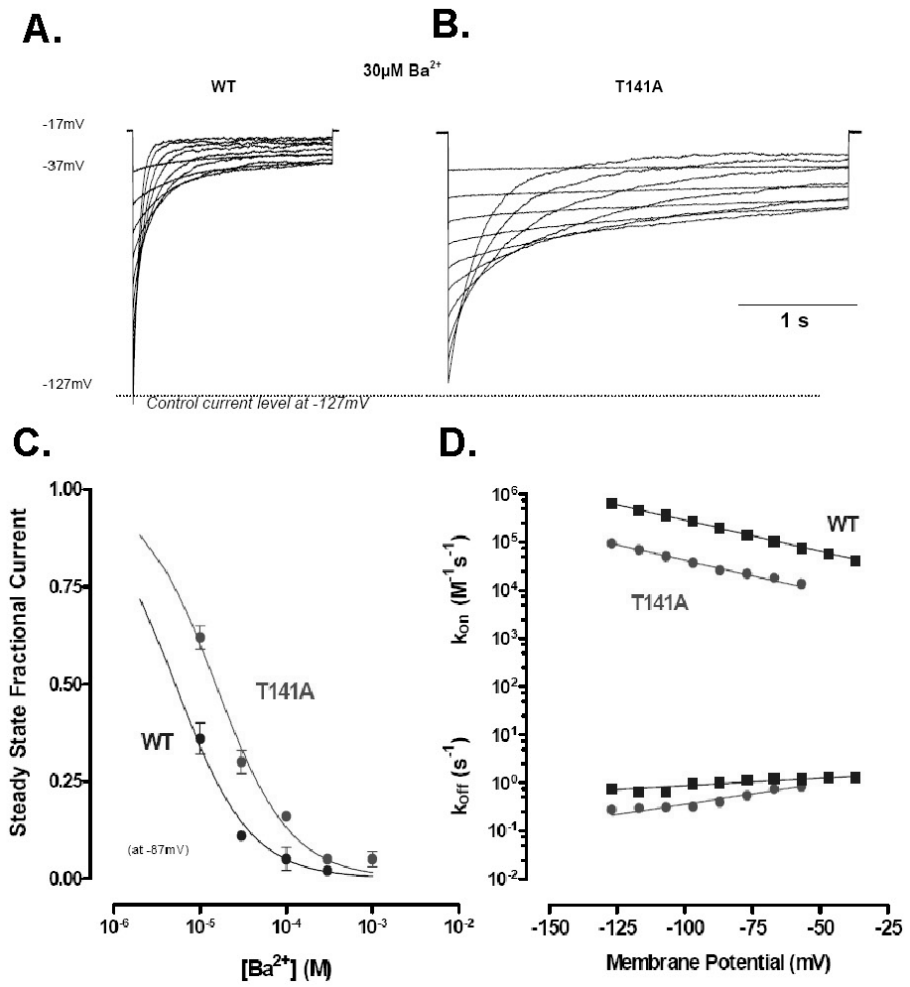

Fig. 4. Ba^{2+} blockage of T141A. T141A slows block and lowers Ba^{2+} affinity (K_d(0)=1.02 mM; δ =0.61), primarily through a reduction in k_{on}. (A, B) Blockage proceeds with a single exponential time course in both the wild type and mutant channel. Kir2.1 currents are shown for wild type (A) and T141A (B) in response to hyperpolarising pulses from a holding potential of −17 mV to voltages between −37 and −127 mV in 10 mV increments. (C) Relationship between the fractional steady state current (ordinate) and $[Ba^{2+}]_o$ (abscissa) for wild type and T141A. (D) Relationship between the transition rate constants k_{on} (above) and k_{off} (below) plotted (ordinate) against membrane potential (abscissa) for wild type and T141A.

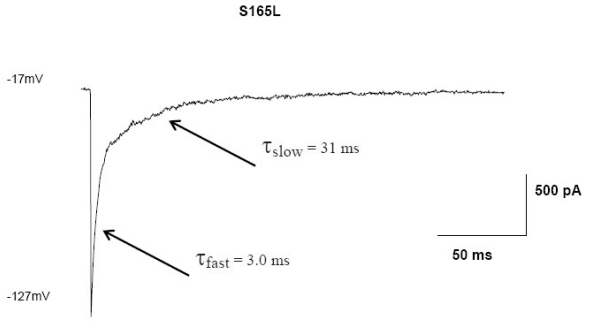

Fig. 5. Ba^{2+} blockage of S165L. S165L reduces Ba^{2+}affinity (K_d(0)=1.04 mM; δ =0.69) and slows blockage. With 300 μM Ba^{2+}, the time-course of block becomes biphasic. The time course of each component and the relatively high affinity for Ba^{2+} makes detailed analysis of kinetics difficult.

et al., 2000a), we also examined the double mutant T141A/S165L, finding that the effects of the individual mutations were much enhanced. We used this mutation once again to allow a more complete dissection of the two components of blockage observed.

Slow and fast components of blockage in T141A/S165L

Ba^{2+} blockage was also enhanced in the double mutant T141A/S165L, and blockage developed with the double exponential time course seen for S165L at $[Ba^{2+}] > 100\ \mu$M (Fig. 6). Using hyperpolarizing pulses of up to 5s duration, it was possible to identify and quantify a fast and slow component within the block over a concentration range of 100 μM to 10 mM. As with S165L, the faster component became more dominant as the concentration of Ba^{2+} increased. By plotting $1/\tau_{fast}$ and $1/\tau_{slow}$ against external Ba^{2+} concentration, values for k_{on} and k_{off} for each component could be generated. These plots showed that the voltage-dependence of Ba^{2+} block in this channel is derived almost entirely from the fast component. This is demonstrated when the values of k_{on} and k_{off} are used as a means of calculating affinity of the channel for Ba^{2+}. A K_d(0) of 65.4 mM with δ =0.60 was obtained for the fast component while K_d(0) for the slow component was 1.77 mM with a δ close to zero (−0.02). The value for the overall K_d(0), calculated from the steady-state fractional current remaining after completion of both the slow and fast components, gave 473 mM (δ =

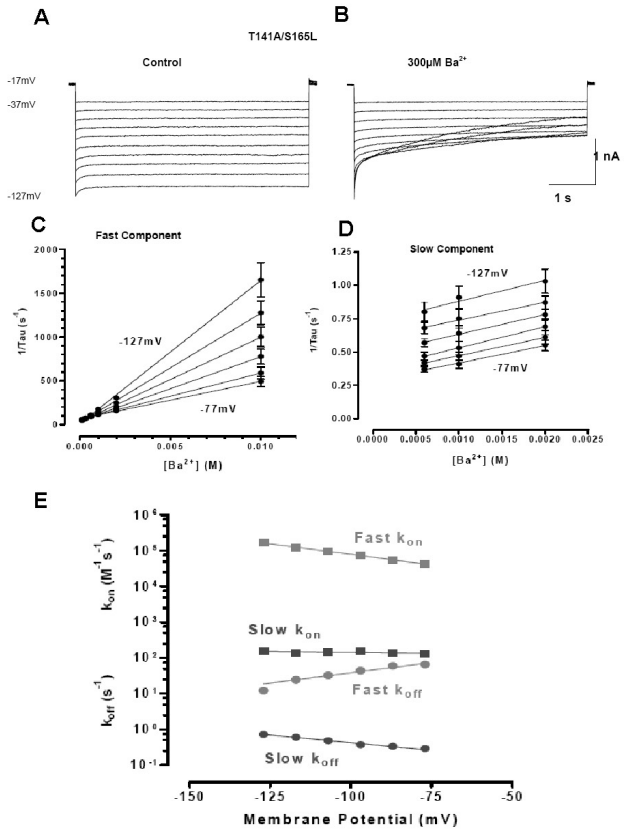

Fig. 6. Ba^{2+} blockage of T141A/S165L. The double mutant T141A/S165L, which is permeable to Rb^{+} and Cs^{+}, drastically reduces Ba^{2+} affinity, revealing two blocking sites. At high concentrations, blockage becomes dominated by the fast component allowing calculation of affinity and voltage- dependence ($K_d(0)$=210 mM; δ=0.68). (A, B) Currents from T141A/S165L mutant channels obtained in the absence (A) and presence of 300 μM Ba^{2+} in response to hyperpolarising pulses from a holding potential of −17 mV to voltages between −37 and −127 mV. (C, D) The time constants obtained by fitting the decline in current with the sum of two exponentials and plotted (ordinates) against Ba^{2+} concentration for fast (C) and slow (D) components. (E) Plots of the transition rate constants (ordinate) k_{on} (symbols in red) and k_{off} (symbols in blue) plotted against membrane potential. k_{on} for the faster component has the greater voltage dependence.

1.08).

D172K and D172R mutants alter blockage by Ba^{2+}

We asked whether the residue D172, which lies in the central cavity of Kir2.1 (Minor et al., 1999; Nishida et al., 2007), contributes significantly to Ba^{2+} blockage. Mutation to Glu (D172E) or Gln (D172Q) had relatively little effect. In 30 μM-Ba^{2+}, blockage occurred at −97 mV with τ=45.2 ± 8.1 ms (n=4) for D172E and 28.4 ± 2.2 ms (n=7) for D172Q, slightly faster than was found with wild type (τ=81.8 ± 19.9 ms; n=5). However, the double mutant D172N-S165L slows blockage about 40-fold, with τ=884 ± 72 ms (n=5) at −97 mV, presumably principally through the effect of the S165L mutation. k_{on} at this voltage was reduced to 9.02×10^3 $M^{-1}s^{-1}$, though its voltage dependence was similar to that in wild-type and in other mutant channels discussed so far.

Fig. 7A, B shows currents in response to voltage steps for wild type channels and for the mutant D172R. Currents in the mutant were still blocked by Ba^{2+} but time required for the blocking reaction to reach steady state was longer than that required for wild type. In 100 μM $[Ba^{2+}]_o$, the time course of blockage follow a single exponential, and the time constant was 415.1 ± 18.3 ms at −97 mV (n=5, mean ± s.e.m; Fig. 7C, D), some 16 fold slower than for wild type.

In Fig. 8A, B the association rate constants are plotted as functions of membrane potential. Both D172R and D172K showed a slowing of blockage giving $k_{on}=6.4\times10^4$ $M^{-1}s^{-1}$ and $k_{on}=1.3\times10^4$ $M^{-1}s^{-1}$ at −127 mV (n=6, mean ± s.e.m). At −127 mV, the reduction of k_{on} in D172K was some 70-fold (Table 1). In Fig. 8C, channels formed from D172R and D172K mutant subunits are shown to have a much reduced affinity for Ba^{2+} as a blocking cation. At 0 mV, the reduction in affinity of D172R and D172K was 16.7 and 24.0 fold: $K_d(0)$ was 1.8 mM (δ=0.49; n=6) in D172R and 2.5 mM (δ=0.42; n=6) in D172K. D172K and D172R mutants decreased affinity for $Ba^{2+}$and reduced the transition rate constant k_{on}. These results indicate that the residue D172 also contributes to the control of Ba^{2+} blockage in Kir2.1.

DISCUSSION

In this study, we have examined the effects of certain mutations of murine Kir2.1 on ionic blockage by Ba^{2+}. The mutant channels T141A, S165L T141A/S165L, D172K and D172R all exhibited a lower affinity for Ba^{2+} with a reduced blocking transition rate constant, k_{on}. The mutant channels S165L and T141A/S165L showed two components of blockage of different affinities and very different time courses. D172K and D172R showed one blocking component.

First we deal with mutation of Y145 in the selectivity filter. Use of the mutant Y145F and of the concatameric dimers WT-Y145L and WT-Y145V (where two of the four Tyr residues in the selectivity filter were replaced) showed little or no change in Ba^{2+} blockage (Fig. 3; Table 1). The lack of alteration in blocking kinetics is independent of whether the dissociation constant at 0 mV, $K_d(0)$, transition rate constants k_{on} and k_{off}, or electrical distance, δ are considered. The result contrasts with that of Lu et al. (2001), who showed amide-to-ester mutation in the selectivity filter decreased binding affinity for both Cs^{+} and Ba^{2+}. The reduction in affinity was particularly striking for mutation of inner glycine (G144) where the reduction in Ba^{2+} affinity was some 6500-fold (Lu et al., 2001). Neither the amide to ester mutations used by Lu et al. (2001) nor our own mutations of Y145 (So et al., 2001) change either ionic selectivity among monovalent cations or unitary conductance.

Their mutation of G144 used by Lu et al. (2001) is associated with a large reduction in channel open time, which might be expected to restrict access of Ba^{2+} to its blocking site, particularly if, as Jiang and MacKinnon (2000) have shown for KcsA, Ba^{2+} blocks at the intracellular end of the selectivity filter, beyond GYG. However the mutant dimer WT-Y145V also has a reduced channel open time, though open time was not reduced in WT-Y145L or in Y145F (So et al., 2001). Indeed the reduction in open time is greater in WT-Y145V than it is in the backbone mutant of G144 (Lu et al., 2001; So et al., 2001). Reduced access to the blocking site is unlikely to explain the difference between our result and that of Lu et al. (2001).

We have tested blockage at the intracellular end of the

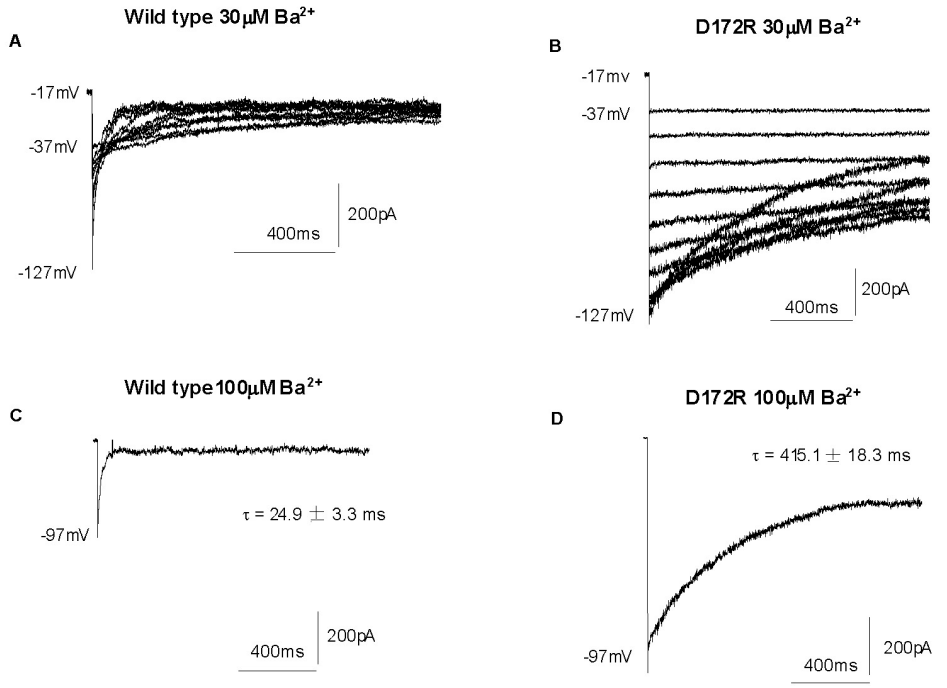

Fig. 7. Ba^{2+} blockage of Kir2.1 wild type and D172R. (A, B) Membrane currents recorded from a single CHO cell expressing the gene for wild type (A) and D172R (B) in response to voltage steps from a holding potential of −17 mV to test potentials ranging from +63 to −127 mV (10 mV increments) in the presence of 30 μM Ba^{2+}. (C, D) Currents in wild type (C) and D172R (D) with 100 μM Ba^{2+} at the voltage indicated. The time dependence of block fitted to a single exponential.

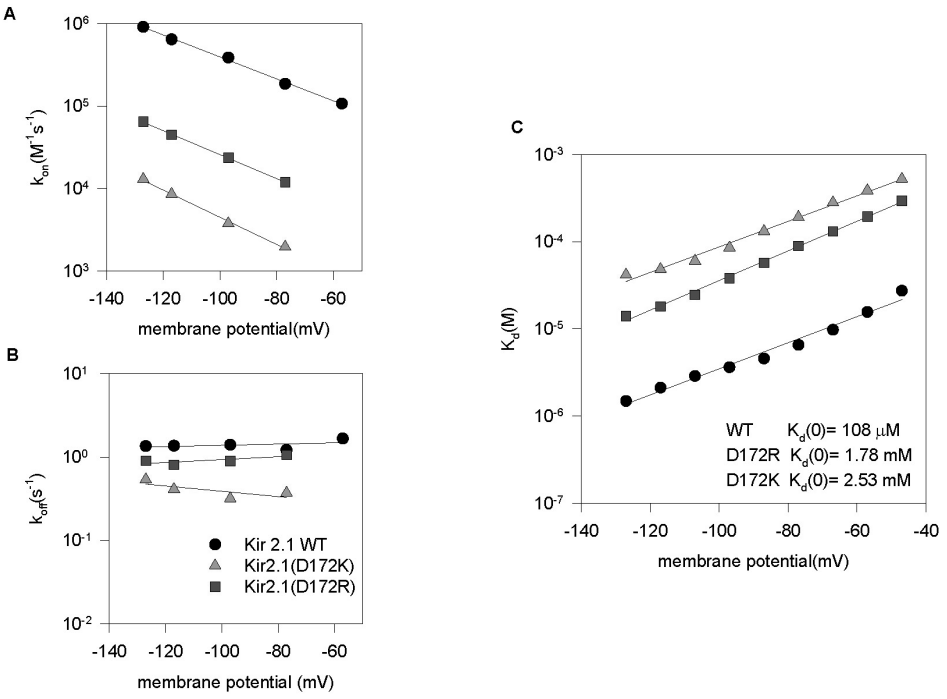

Fig. 8. D172K and D172R mutants decreased k_{on} and increased the K_d. (A) Plot of k_{on} against membrane potential for wild type (circles), D172R (squares), D172K (triangles). k_{on} values were obtained from τ by fitting regression lines to Eqn (3) of the text. (B) Plot of k_{off} against membrane potential for wild type (circles), D172R (squares) and D172K (triangles). k_{off} values were obtained using K_d and k_{on}. (C) K_d values obtained from the concentration-dependent inhibition of the steady-state currents were plotted against membrane potentials. The solid line is the best fit of the data obtained at membrane potential (V) ranging from −127 mV to −47 mV, using the Woodhull equation (Eqn 4 of the text). The values obtained for $K_d(0)$ and δ are summarized in Table 1.

filter by making mutations of T141 (and S165; see below). The blocking site identified by Jiang and MacKinnon (2000) is likely to be formed in Kir2.1 by the backbone carbonyl oxygen and the side chain hydroxyl of T142 (Nishida et al., 2007), but we have not examined alterations of this residue. However, T141 will lie close to this site and is likely to help stabilise it structurally. And our results show a substantial alteration in blocking kinetics as a result of the alteration T141A.

In our results, $K_{d(0)}$ was increased in T141A to 858 ± 62 μM The principal change was a reduction in k_{on} for the blocking reaction (Fig. 6; Table 1): k_{off} was reduced to a lesser extent (Fig. 6). Our results show only small differences from those of Alagem et al. (2001). Using oocyte expression and working with higher $[K^{+}]_o$, they found a $K_d(0)$ of 320 ± 18 μM for T141A. In their experiments, k_{on} was altered, but k_{off} was not. Our results are also consistent with those of Zhou et al. (1996), who showed in Kir1.1 that the mutant V121T

− V121 lies in Kir1.1 at the site equivalent to T141 in Kir2.1 − increases Ba^{2+} affinity, with effects on both the blocking and unblocking rates. Similarly, in *Shaker* K^+ channels (Hurst et al., 1996; Harris et al., 1998) the mutation of the threonine at position 441, which is located in the corresponding position to T141 in Kir2.1, also affected the Ba^{2+} affinity. From our results, the residue T141 is involved in the stabilization of the Ba^{2+} in its binding site.

Thompson et al. (2000a) showed that S165L reduced the affinity for blockage by Cs^+ and abolished Rb^+ blockage; the effects of dual mutation T141A/S165L were much great than those of either mutation alone. Here, similar results were found for Ba^{2+} blockage. Replacement of Ser165 with Leu (S165L) also alters blockage by Ba^{2+} and the double mutant T141A/S165L in Kir2.1 also further radically reduces the affinity for Ba^{2+}.

Thompson et al. (2000a) argued that S165 was likely a pore lining residue and that changes of T141 and S165 affected affinity independently of each other. Studies of the structure of a Kir3.1/prokaryotic Kir channel chimera are consistent with the hypothesis that S165 lies at the back of the selectivity filter in Kir2.1, helping to stabilise it (Nishida et al., 2007). Further, the fact that the change in affinity is so much greater for the dual mutant, suggests that, far from acting independently of each other (Thompson et al., 2000a), the two residues interact. A coupling ratio (see for example Hidalgo and MacKinnon, 1995) can be computed from the expression

$$\Omega = \frac{K_d(0)_{T141(WT)/S165(WT)} \times K_d(0)_{T141A/S165L}}{K_d(0)_{T141A/S165(WT)} \times K_d(0)_{T141(WT)/S165L}},$$

where the subscripts for the various $K_d(0)$ indicate whether the residues, normally T141 and S165, are in the unaltered (*WT*) or mutant form. This ratio has a value unity in the absence of coupling. In fact the ratio evaluates (using the values for $K_d(0)$ given in Table 1) to 57, strongly indicating coupling. It is likely that both residues stabilise the K^+ coordination site at which Ba^{2+} blocks (Jiang and MacKinnon, 2000).

The blocking process occurs with a double exponential time course in S165L and T141A/S165L, suggestive of more than one blocking site. Since one of these sites, revealed by the reduced affinity caused by mutations S165L and T141A/S165L, appears to have an affinity that lacks voltage dependence (see Results), it is likely that that this (normally lower affinity) site lies at the outer mouth of the channel. Indeed the interaction of divalent cations with Kir channels has for some time been thought to occur via two distinct binding sites; a shallow site that barely senses the membrane electric field, and a deeper one located approximately half-way within the membrane voltage field. Evidence supporting this suggestion come from the works of many researchers (Standen and Stanfield, 1978; Shioya et al., 1993; Reuveny et al., 1996; Sabirov et al., 1997; Shieh et al., 1998) in which channel block by extracellular Mg^{2+} and Ca^{2+} was found to occur through the shallow site, whereas blockage by Ba^{2+} and Sr^{2+} was mediated through the deeper one. Mutants of T141 and S165 affect the deeper binding site, whereas the residues R148 or E125, at the outer mouth of the channel (Navaratnam et al., 1995; Doring et al., 1998; Krapivinsky et al., 1998; Topert et al., 1998), are likely to form the shallow site. Alagem et al (2001) also dissected two sites, one at the outer mouth, at E125 (Alagem et al., 2001).

Jiang and MacKinnon (2000) (see also Neyton and Miller, 1988a, b) argued that K^+ occupancy of the central cavity of KcsA would lock Ba^{2+} into its blocking site. Our results with mutants of D172, whose side chain is exposed in this central cavity are consistent with this prediction. Conservative mutations of D172 (to E and Q) have little effect; however more drastic changes, replacing the negatively charged Asp by the basic residues Lys or Arg, affected channel blockage by Ba^{2+}. Such mutation (D172K, R) reduced the affinity for Ba^{2+} by more than 15-fold and reduced k_{on}. The values for δ of D172K (0.42) and D172R (0.49) are similar to that found in WT (0.43); blockage occurred with first order kinetics in these mutants.

Our results, and those of others (Zhou et al., 1996; Alagem et al., 2001), are consistent with what has been found by Jiang and MacKinnon (2000) using X-ray crystallography. Ba^{2+} was found bound at the intracellular end of the selectivity filter, in the innermost K^+ coordination site. Outer K^+ coordination sites must be traversed by the blocking Ba^{2+} to reach this site. This is less surprising that it may initially seem since: i) Ba^{2+} has a crystalline ionic radius almost identical to that of K^+ (1.35 versus 1.33Å) and ii) it is known that size, rather than charge density determines ability to permeate the K^+ channel selectivity filter (Lockless et al., 2007). K^+ occupancy of the filter may enhance blockage, K^+ coordination sites 1∼3 acting as external lock-in and enhancement sites (see also Neyton and Miller, 1988a, 1988b; Jinag and MacKinnon, 2000; Nishida et al., 2007). The K^+ coordination site in the central cavity (site 5 in Nishida et al., 2007) may act as internal lock-in site. Reduced occupancy here by K^+, as in D172K and R, would be expected to reduce Ba^{2+} affinity, and this is what we find.

We thus suggest that several residues in Kir2.1 help regulate channel blockage by Ba^{2+} either affecting channel structure at the blocking site itself (T141, S165), or affecting occupancy by K^+ at sites where K^+ prevents Ba^{2+} escaping from its site of blockage. These residues will include those that line the selectivity filter and D172 in the central cavity.

ACKNOWLEDGEMENT

We thank The Wellcome Trust, SNU (800-20000229, 800-20000125) and BK21 Human Life Science for support.

REFERENCES

Abrams CJ, Davies NW, Shelton PA, Stanfield PR. The role of a single aspartate residue in ionic selectivity and block of a murine inward rectifier K^+ channel Kir2.1. *J Physiol* 493: 643−649, 1996.

Alagem N, Dvir M, Reuveny E. Mechanism of Ba^{2+} block of a mouse inwardly rectifying K^+ channel: differential contribution by two discrete residues. *J Physiol* 534: 381−393, 2001.

Dart C, Leyland ML, Barrett-Jolley R, Shelton PJ, Spencer PJ, Conley EC, Sutcliffe MJ, Stanfield PR. The dependence of Ag^+ block of a potassium channel, murine Kir2.1, on a cysteine residue in the selectivity filter. *J Physiol* 511: 15−24, 1998.

Doring F, Derst C, Wischmeyer E, Karschin C, Schneggenburger R, Daut J, Karschin A. The epithelial inward rectifier channel Kir7.1 displays unusual K^+ permeation properties. *J Neurosci* 18: 8625−8636, 1998.

Doyle DA, Morais CJ, Pfuetzner RA, Kuo A, Gulbis JM, Cohen SL, Chait BT, Mackinnon R. The structure of the potassium channel: molecular basis of K^+ conduction and selectivity. *Science* 280:

69−77, 1998.

Duprat F, Lesage F, Fink M, Reyes R, Heurateaux C, Lazdunski M. TASK, a human background K^+ channel to sense external pH variations near physiological pH. *EMBO J* 17: 5464−5471, 1997.

Fakler B, Brandle U, Bond CH, Glowatzki E, Konig C, Adelman JP, Zenner HP, Ruppersberg JP. A structural determinant of differential sensitivity of cloned inward rectifier K^+ channels to intracellular spermine. *FEBS Lett* 356: 199−203, 1994.

Fakler B, Brandle U, Glowatzki E, Weidemann S, Zenner HP, Ruppersberg JP. Strong voltage-dependent inward rectification of inward rectifier K^+ channels is caused by intracellular spermine. *Cell* 80: 149−154, 1995.

Ficker E, Taglialatela M, WIBLE BA, Henley CM, Brown AM. Spermine and spermidine as gating molecules for inward rectifier K^+ channels. *Science* 266: 1068−1072, 1994.

Hagiwara S, Miyazaki S, Moody W, Patlak J. Blocking effects of barium and hydrogen ions on the potassium current during anomalous rectification in the starfish egg. *J Physiol* 279: 167−185, 1978.

Hagiwara S, Yoshii M. Effects of internal potassium and sodium on the anomalous rectification of the starfish egg as examined by internal perfusion. *J Physiol* 292: 251−265, 1979.

Harris RE, Larsson HP, Isakoff EY. A permanent ion binding site located between two gates of the Shaker K^+ channel. *Biophys J* 74: 1808−1820, 1998.

Heginbotham L, Lu Z, Abramson T, Mackinnon R. Mutations in the K^+ channel signature sequence. *Biophys J* 66: 1061−1067, 1994.

Hidalgo P, Mackinnon R. Revealing the architecture of a K^+ channel pore through mutant cycles with a peptide inhibitor. *Science* 268: 307−310, 1995.

Hurst RS, Toro L, Stefani E. Molecular determinants of external barium block in Shaker potassium channels. *FEBS Lett* 388: 59−65, 1996.

Jiang Y, Mackinnon R. The barium site in a potassium channel by x-ray crystallography. *J Gen Physiol* 115: 269−272, 2000.

Krapivinsky G, Medina I, Eng L, Krapivinsky L, Yang Y, Clapham DE. A novel inward rectifier K^+ channel with unique pore properties. *Neuron* 20: 995−1005, 1998.

Kunkel TA. Rapid and efficient site-specific mutagenesis without phenotypic selection. *Proc Natl Acad Sci USA* 82: 488−492, 1985.

Kuo A, Gulbis JM, Antcliff JF, Rahman T, Lowe ED, Zimmer J, Cuthbertson J, Ashcroft FM, Ezaki T, Doyle DA. Crystal structure of the potassium channel KirBac1.1 in the closed state. *Science* 300: 1922−1926, 2003.

Lancaster MK, Dibb KM, Quinn CC, Leach R, Lee JK, Findlay JB, Boyett MR. Residues and mechanisms for slow activation and Ba^{2+} block of the cardiac muscarinic K^+ channel, Kir3.1/Kir3.4. *J Biol Chem* 275: 35831−35839, 2000.

Lee YM, Yang DK, Ashmole I, Stanfield PR, So I, Kim KW. Residues lining the pore region of the murine inward rectifier K^+ channel (KIR2.1) control Ba^{2+} blockage. *Biophysical J* 80: 631A, 2001.

Leech CA, Stanfield PR. Inward rectification in frog skeletal muscle fibres and its dependence on membrane potential and external potassium. *J Physiol* 319: 295−309, 1981.

Lesage F, Guillemare E, Fink M, Duprat F, Lazdunski M, Romely G, Barhanin J. TWIK-1, a ubiquitous human weakly inward rectifying K^+ channel with a novel structure. *EMBO J* 15: 1004−1011, 1996.

Lockless SW, Zhou M, Mackinnon R. Structural and thermodynamic properties of selective ion binding in a K^+ channel. *PLoS Biology* 5: 1079−1088, 2007.

Lopatin AN, Makhina EN, Nichols CG. Potassium channel block by cytoplasmic polyamines as the mechanism of intrinsic rectification. *Nature* 372: 366−369, 1994.

Lopatin AN, Makhina EN, Nichols CG. The mechanism of inward rectification of potassium channels: "long-pore plugging" by cytoplasmic polyamines. *J Gen Physiol* 106: 923−955, 1995.

Lopatin AN, Nichols CG. [K^+] Dependence of polyamine-induced rectification in inward rectifier potassium channels (IRK1, Kir2.1). *J Gen Physiol* 108: 105−113, 1996.

Lu T, Ting AY, Mainland J, Jan LY, Schultz PG, Yang J. Probing ion permeation and gating in a K^+ channel with backbone mutations in the selectivity filter. *Nature Neurosci* 4: 239−246, 2001.

Matsuda H, Saigusa A, Irisawa H. Ohmic conductance through the inwardly rectifying K channel and blocking by internal Mg^{2+}. *Nature* 325: 156−159, 1987.

Minor DL, Masseling SJ, Jan YN, Jan LY. Transmembrane structure of an inwardly rectifying potassium channel. *Cell* 96: 879−891, 1999.

Navaratnam DS, Escobar L, Covarrubias M, Oberholtzer JC. Permeation properties and differential expression across the auditory receptor epithelium of an inward rectifier K^+ channel cloned from the chick inner ear. *J Biol Chem* 270: 19238−19245, 1995.

Neyton J, Miller C. Potassium blocks barium permeation through a calcium-activated potassium channel. *J Gen Physiol* 92: 549−567, 1988a.

Neyton J, Miller C. Discrete Ba^{2+} block as a probe of ion occupancy and pore structure in the high conductance Ca^{2+} activated K^+ channel. *J Gen Physiol* 92: 569−586, 1988b.

Nishida M, Cadene M, Chait BT, Mackinnon R. Crystal structure of a Kir3.1-prokaryotic Kir channel chimera. *EMBO J* 26: 4005−4015, 2007.

Reuveny E, Jan YN, Jan LY. Contributions of a negatively charged residue in the hydrophobic domain of the IRK1 inwardly rectifying K^+ channel to K^+-selective permeation. *Biophys J* 70: 754−761, 1996.

Sabirov RZ, Tominaga T, Miwa A, Okada Y, Oiki S. A conserved arginine residue in the pore region of an inward rectifier K channel (IRK1) as an external barrier for cationic blockers. *J Gen Physiol* 110: 665−677, 1997.

Shieh RC, Chang JC, Arreola J. Interaction of Ba^{2+} with the pores of the cloned inward rectifier K^+ channels Kir2.1 expressed in Xenopus oocytes. *Biophys J* 75: 2313−2322, 1998.

Shioya T, Matsuda H, Noma A. Fast and slow blockades of the inward-rectifier K^+ channel by external divalent cations in guinea-pig cardiac myocytes. *Pflügers Arch* 422: 427−435, 1993.

So I, Ashmole I, Davies NW, Sutcliffe MJ, Stanfield PR. The K^+ channel signature sequence of murine Kir2.1: mutations that affect microscopic gating but not ionic selectivity. *J Physiol* 531: 37−50, 2001.

So I, Ashmole I, Soh H, Park CS, Spencer PJ, Leyland M, Stanfield PR. Intrinsic gating in inward rectifier potassium channels (Kir2.1) with low polyamine affinity generated by site directed mutagenesis. *Kor J Physiol Pharmacol* 7: 131−142, 2003a.

So I, Ashmole I, Stanfield PR. The substates with mutants that negatively charged aspartate in position 172 was replaced with positive charge in murine inward rectifier potassium channel (murine Kir2.1). *Kor J Physiol Pharmacol* 7: 267−273, 2003b.

Standen NB, Stanfield PR. A potential- and time-dependent blockade of inward rectification in frog skeletal muscle fibres by barium and strontium ions. *J Physiol* 280: 169−191, 1978.

Stanfield PR, Davies NW, Shelton PA, Sutcliffe MJ, Khan IA, Brammar WJ, Conley EC. A single aspartate residue is involved in both intrinsic gating and blockage by Mg^{2+} of the inward rectifier, IRK1. *J Physiol* 478: 1−6, 1994.

Stanfield PR, Nakajima S, Nakajima Y. Constitutively active and G-protein coupled inward rectifier K^+ channels: Kir2.0 and Kir3.0. *Rev Physiol Biochem Pharmacol* 145: 47−179, 2002.

Thompson GA, Passmore GM, Spencer PJ, Davies NW, Stanfield PR. Blockage of inward rectifier potassium channels (murine Kir2.1) by Ba^{2+} is influenced by an aspartate residue (D172). *J Physiol* 511P: 146P, 1998.

Thompson GA, Leyland ML, Ashmole I, Sutcliffe MJ, Stanfield PR. Residues beyond the selectivity filter of the K^+ channel Kir2.1 regulate permeation and block by external Rb^+ and Cs^+. *J Physiol* 526: 231−240, 2000a.

Thompson GA, Leyland ML, Ashmole I, Stanfield PR. Residues in H5 and M2 of murine Kir2.1 regulate Ba^{2+} block. *J Physiol*

526P: 10S, 2000b.

Topert C, Doring F, Wischmeyer E, Karschin C, Brockhaus J, Ballanyi K, Derst C, Karschin A. Kir2.4: a novel K^+ inward rectifier channel associated with motoneurons of cranial nerve nuclei. *J Neurosci* 18: 4096−4105, 1998.

Woodhull AM. Ionic blockage of sodium channels in nerve. *J Gen Physiol* 61: 687−708, 1973.

Yang J, Jan YN, Jan LY. Determination of the subunit stoichiometry of an inwardly rectifying potassium channel. *Neuron* 15: 1441−1447, 1995.

Zhou H, Chepilko S, Schutt W, Choe H, Palmer LG, Sackin H. Mutations in the pore region of ROMK enhance Ba^{2+} block. *Am J Physiol* 271: C1949−C1956, 1996.